IRAQI BULLETIN OF GEOLOGY AND MINING (IBGM)\
IRAQ GEOLOGICAL SURVEY (GEOSURV-IRAQ)

*IBGM (**2025**, Vol 21; Issue 2)* 457-471

STRATIGRAPHIC AND GEOCHEMICAL INSIGHTS OF CLAY BEDS IN THE EOCENE SUCCESSION, NORTHERN IRAQ

Mohammed Sattam Abbas[1] and Enaam J. Abdullah[2]

[1] Department of Geophysics, College of Remote Sensing and Geophysics, Al-Karkh University of Science, Baghdad, Iraq; e-mail: moh.sattam@kus.edu.iq, orcid.org/0000-0001-8857-2430
[2] Department of Geology, College of Science, University of Baghdad. e-mail: anam.g@sc.uobaghdad.edu.iq, orcid.org/0000-0001-5267-3539

Type of the Paper (Article)
Received: 20/01/2025
Accepted: 17/10/2025
Available online: 27/12/2025

Abstract

The red and grey mudstone, which was interbedded in the middle of the Eocene layers (between the Gercus and Pila Spi Formation) in northeastern Iraq, was studied to determine the origin of the rocks, the climate that existed then, the intensity of the weathering process back then, and the way the plates of the earth moved when the rocks were being formed. As per the study of the X-Ray Fluorescence, the data indicate that MgO and CaO have more value compared to the Archean Australian Shale (PAAS) and North American Shale Composite (NASC); however, the amounts of other oxides are lesser. The associations of the key oxides indicate a combination of rocks of their formation, with most being mafic, and a few being intermediate and felsic igneous rocks, and indicating that they were formed along both the stable and unstable continental boundaries. Yet, the samples of clay were strongly chemically weathered, and the degree to which the chemicals were developed in the region of their origin, and this suggests that the past climate was more wet or more dry, which suggests that the layers of the material were not moved long distances, because the element ratios suggest that these rocks were not oxidized, or were oxidized, and that they may have been moved long distances in the conditions under which they were deposited being such that were either more or less oxygen-deprived, or were entirely oxidized, and which could have been caused.

Keywords: Stratigraphic analysis, Geochemistry, Paleo-environment, Ancient climate, Clay beds, Eocene.

1. Introduction

Through analyzing the chemical composition of the sedimentary rocks, chemostratigraphy tends to infer the sedimentary environment and ecological environment of the past. It does so by examining changes in elemental ratios in order to identify changes in the sedimentary settings. The process will also be able to show historic climatic changes and set correlations

ISSN 1811-4539, EISSN 3005-3714
https://doi.org/10.59150/ibgm2102a25
IBGM: http://ibgm-iq.org/
Academic Scientific Journals: www.iasj.net

between strata in different regions. The use of chemostratigraphy helps in particular the reconstruction of the past deposition and climatic patterns, which supplements the geological interpretation via biostratigraphy and lithostratigraphy (Armstrong-Altrin et al., 2017).

Geochemistry of sediments, which are a product of weathered rocks, can indicate the nature of (Hayashi et al., 1997) the rocks that formed the sediments, the environment in which the sediments were also deposited many years ago, the climate at that time, and the tectonic environment (Hayashi et al., 1997). The geochemical indicators in the sedimentary rocks play a vital role in establishing the tectonic conditions and the level of weathering that took place in the past (Roser & Korsch, 1986).

The bedrock composition is also connected to the original source of rocks and the influence of the diagenetic processes, and this is why it is applicable in several ways, because of the stability and minimal mobility of some of the elements. The concentrations of immobile elements vary in a broad way in various source rocks (e.g., felsic or basic) of various tectonic environments (Wronkiewicz & Kent C, 1989).

The study aims to explain the nature of the tectonic setting, the sedimentary environment, and the origin of the clay layers that exist between the Gercus and Pila Spi Formations in north Iraq using the chemical properties of the major and trace elements.

2. Geological Setting

The Gercus and Pila Spi Formations are revealed in the much-twisted area found in the north of Iraq. The beds of mudstone are very evident towards the lower portion of the Pila Spi Formation, as compared with the clastic division in the upper portion of the Gercus Formation. This higher section is much eroded in the high ridges of the High Folded Zone in the Unstable Shelf in the whole of northern Iraq. The superior section of this formation is of medium to thick, even beds of mudstones, between which are spread thin beds of siltstones, white marl lenses, and chert nodules at the top. The bottom is made up of a fossil-bearing, homogenous, hard, porous, or vitreous, bituminous, white limestone that is uniform and porous. This series depicts a superficial lagoonal setting (Jassim & Goff, 2006). The Pila Spi Formation is made up of a series of limestone and marly limestone approximately 240 m thick. The lower limit of the formation with the Avanah Formation is marked by a lithological transition in the limestone that is massive limestone layers with chert nodules to bedding that is thickly lithified of grey color, separated by thinner marl layers, to form a continuous contact. The occurrence of basal conglomerate is used to define the upper limit of the Fatha Formation, which implies the presence of an erosion unconformity surface (Fendakly, 2011).

3. Study Area Location

The investigated area is located within the northeastern part of Iraq, specifically in the Kurdistan region, within the city of Erbil. This area marks the transitional zone between highly folded and gently folded terrains. Here, layers of clay are exposed, nestled between the Gercus Formation and the Pila Spi Formation. The study encompasses two distinct sections: Section A, located near the village of Bardin with coordinates (N36°39'52.1678" E44°14'01.4889"), and Section B, situated near the village of Ashkafta with coordinates (N36°36'49.6861" E44°17'55.7037"), as illustrated in Figures (1, 2, 3, and 4).

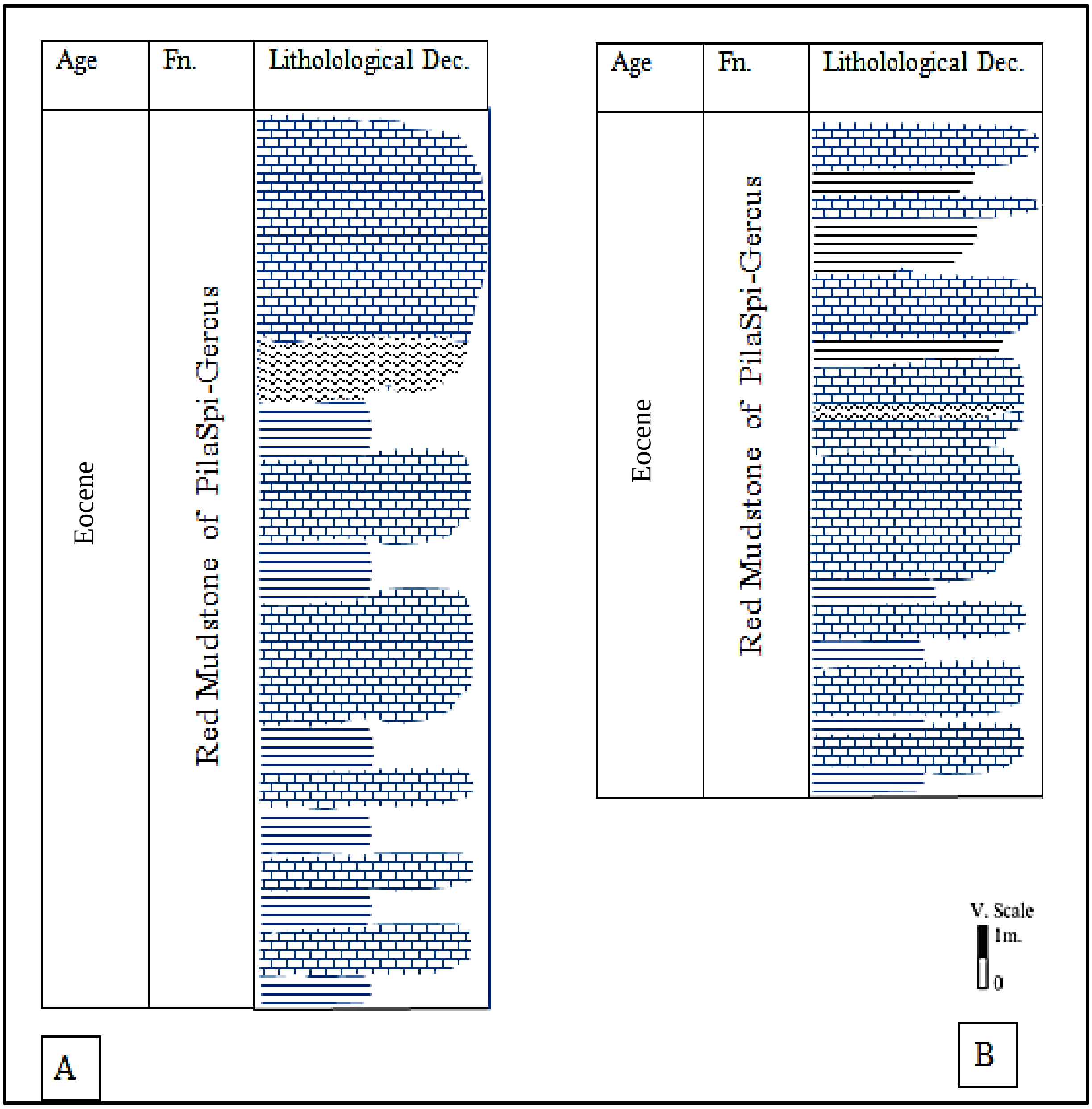

Figure 1. Stratigraphic column of the sections A and B.

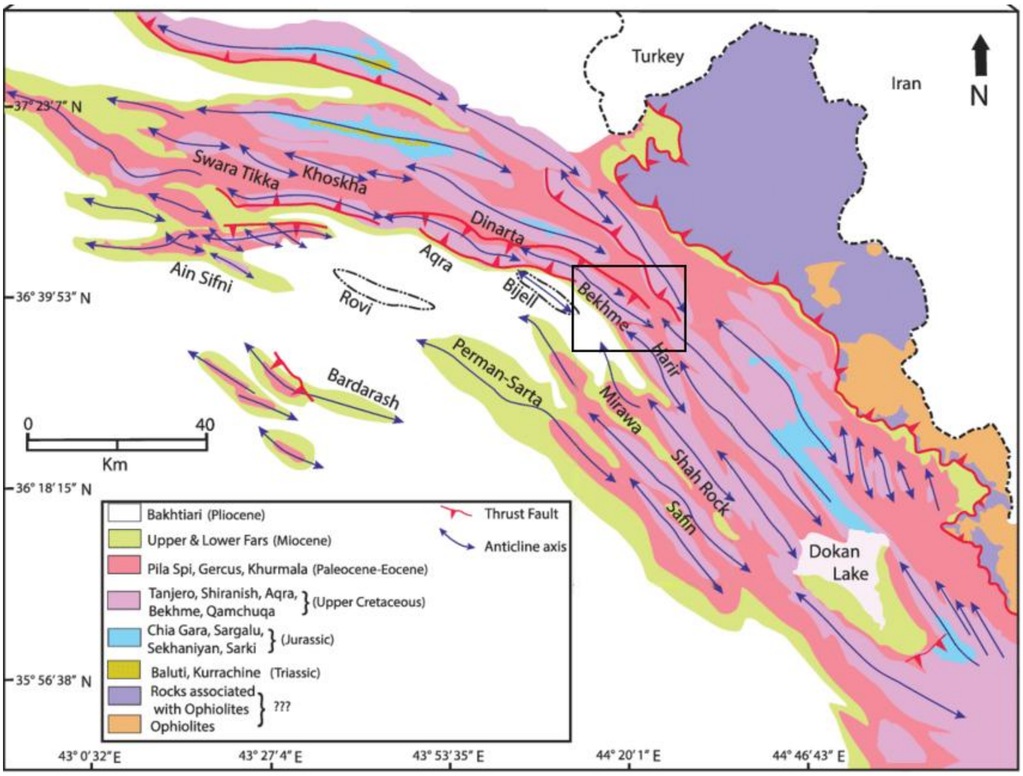

Figure 2. Geological map of the study area (after Sissakian & Fouad, 2016).

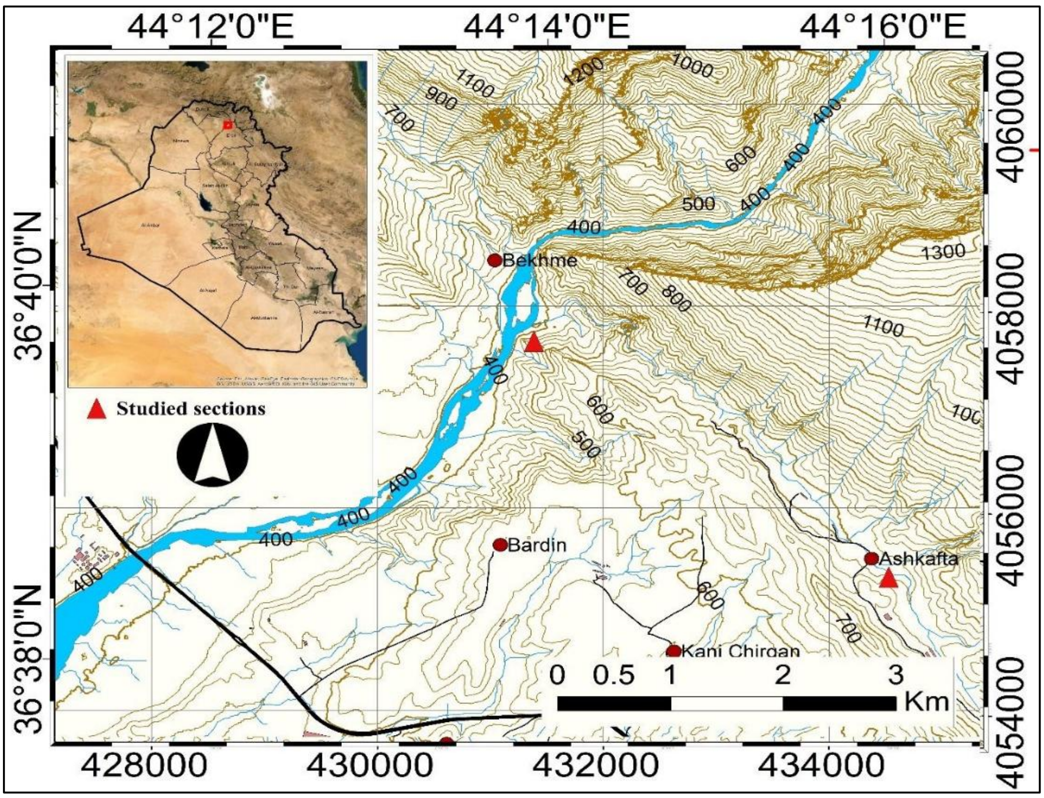

Figure 3. The location map of the study site highlighted the studied section in red triangles.

Figure 4. Field images: a) for site A near Bardin, and b) for Section B, near the village of Ashkafta.

4. Materials and methods

The field research involved selecting the most suitable and accessible clay layers that are interleaved within the Pilaspi Formation. A total of 12 representative clay samples were carefully chosen from these two sections. A clearly exposed section was specifically chosen for this study. Section A was observed in the field to transition from a 3 – 4-meter-thick layer of carbonate limestone belonging to the Pila Spi Formation to the reddish, clastic sediments of the Gercus Formation, with alternating layers of clay beds measuring (2 – 1.5) meters in thickness (Figure 4a &b). Section B was noted in the field to shift from a (2 – 4) meter thick limestone layer of the Pila Spi Formation to the red, clastic sediments of the Gercus Formation, which includes a 1-meter-thick clay bed layer (Figure 4c and d).

The determination of major oxide elements and certain trace elements was performed using XRF analysis at the Iraqi-German laboratory, which is part of the Department of Earth Sciences at Baghdad University. The preparation of the samples followed the procedures outlined in (Abubakar et al., 2019). The XRF spectrometer's material analysis mode is adept at analyzing a broad spectrum of materials, ranging from aluminum (Z = 13) to uranium (Z = 92). The equipment can accurately detect material compositions ranging from 0.1% to 100% (Neikov et al., 2018).

5. Results

5.1. Major oxides geochemistry

The geochemical compositions of the major oxides found in the clay beds are presented in Table 1. The average percentages of oxides in the examined rock samples are detailed in Table 1, organized from the highest to lowest percentages in both sections, as follows: SiO_2, CaO, MgO, Al_2O_3, and Fe_2O_3. When compared to the average shale compositions of the North American Shale Composite (NASC) (Gromet et al., 1984) and the Post-Archean Australian Shale (PAAS) (Taylor & McLennan, 1985), the results indicate that MgO and CaO levels are higher than the specified limits, while the values of the other oxides are lower.

Table 1. Main contents of clay bed samples (wt%).

Sample No.	SiO_2	Al_2O_3	*MgO*	Fe_2O_3	*CaO*	TiO_2	K_2O	P_2O_5	Na_2O	*MnO*
1A	38.3	8.27	9.91	5.28	15.58	0.49	0.94	0.07	0.61	0.03
2A	33.98	10.38	8.11	6.23	17.92	0.46	1.16	0.16	0.98	0.11
3A	31.07	9.34	7.09	6.38	15.99	1.00	0.92	0.14	1.20	0.11
4A	34.12	7.82	9.92	6.71	15.88	0.67	0.07	0.32	0.79	0.07
5A	17.9	6.43	12.36	2.04	25.31	0.28	0.45	0.04	0.80	0.05
6A	15.23	2.66	13.80	2.20	24.83	0.18	0.42	0.05	0.65	0.06
Average	**28.43**	**7.48**	**10.20**	**4.81**	**19.25**	**0.51**	**0.66**	**0.13**	**0.84**	**0.07**
1B	33.4	8.99	8.23	4.42	14.99	0.78	0.25	0.48	1.40	0.01
2B	20.58	8.64	9.32	2.49	26.07	0.57	1.11	0.15	0.98	0.12
3B	36.81	10.88	8.13	3.21	11.45	0.61	0.16	0.33	0.85	0.01
4B	30.01	8.41	10.42	3.84	16.87	0.31	0.65	0.06	0.69	0.06
5B	15.76	2.80	13.58	1.91	26.24	0.22	0.48	0.02	0.44	0.02
6B	45.19	6.89	8.57	6.53	4.91	0.59	1.34	0.04	0.27	0.02
Average	**30.29**	**7.77**	**9.71**	**3.73**	**16.76**	**0.51**	**0.67**	**0.18**	**0.77**	**0.04**
PAAS	62.4	18.78	2.19	7.18	1.29	0.99	3.68	0.16	1.19	
NASC	64.82	17.05	2.83	5.7	3.51	0.8	3.97	0.15	1.13	

5.2. Trace elements geochemistry

The concentrations of minor elements are presented in Table 2. The sequence of minor elements in section A is as follows: Mn > Cr > Sr > Ni > Zn >V > Zr > Cu > Rb > Co > Th > U, while section B shows minor variation in the sequence: Sr >Mn >Cr >Ni >V >Zn >Zr >Rb > Co > Th > U.

Table 2. Minor elements concentrations (ppm).

No.	*V*	*Cr*	*Mn*	*Co*	*Ni*	*Cu*	*Zn*	*Rb*	*Sr*	*Zr*	*Th*	*U*
1A	151.80	335.74	202.83	11.95	224.59	15.02	40.01	33.19	92.25	64.55	3.9	1
2A	71.70	362.49	879.01	16.28	217.84	35.95	79.54	43.43	404.03	125.33	4.9	1
3A	149.56	574.93	882.88	16.28	198.66	34.03	78.57	41.33	396.84	135.40	4	0.6
4A	84.59	289.90	525.86	7.86	117.56	76.37	485.19	40.97	323.02	130.96	6.9	1
5A	54.34	721.15	407.67	3.07	174.30	13.10	30.85	17.01	589.97	1.04	1	2.29
6A	112.59	150.25	440.74	7.39	148.68	103.53	40.97	14.72	456.37	15.62	0.8	1
AVG	**104.10**	**405.74**	**556.50**	**10.47**	**180.27**	**46.33**	**125.85**	**31.78**	**377.08**	**78.82**	**3.58**	**1.15**
1B	185.41	97.36	79.54	6.06	48.17	14.78	133.69	22.95	119.23	107.86	6.9	4.3
2B	98.59	438.57	903.02	25.95	213.36	35.71	83.87	43.43	413.16	122.15	5.1	1
3B	129.96	94.69	82.71	3.07	37.80	18.13	72.15	17.19	125.23	85.58	6	2.2
4B	84.59	244.94	497.67	13.29	313.24	18.61	44.91	24.05	910.71	21.91	1	1
5B	128.84	276.49	162.48	3.07	77.88	76.45	27.56	16.73	93.44	28.58	2.4	1
6B	322.10	535.46	169.99	36.02	459.09	38.82	89.66	57.88	744.80	55.67	0.7	2.8
AVG	**158.25**	**281.25**	**315.90**	**14.58**	**191.59**	**33.75**	**75.31**	**30.37**	**401.09**	**70.29**	**3.68**	**2.05**

5.3. Provenance

Ratios of key elements are often used as indicators to determine the origin and parent rocks (Armstrong-Altrin et al., 2017).

Discriminant functions established by Roser and Korsch (1988) are based on the concentrations of TiO_2, total Fe_2O_3, MgO, Na_2O, and K_2O, where F1 = 30.638 TiO_2/ Al_2O_3 − 12.541 $Fe_2O3(t)$/ Al_2O_3 + 7.329 MgO/ Al2O3 + 12.031 Na_2O/ Al_2O_3 + 35.402 K_2O/ Al2O3 − 6.382; F2 = 56.500 TiO_2/ Al_2O_3 − 10.879 $Fe_2O_3(t)$/ Al2O_3 + 30.875 MgO/ Al_2O_3 − 5.404 Na_2O/ Al_2O_3 + 11.112 K_2O/ Al_2O_3 − 3.89) (Figure 5). The claystone samples from both sections plot within the range of mafic to intermediate igneous origins, while two samples fall into the field of quartz sedimentary origin.

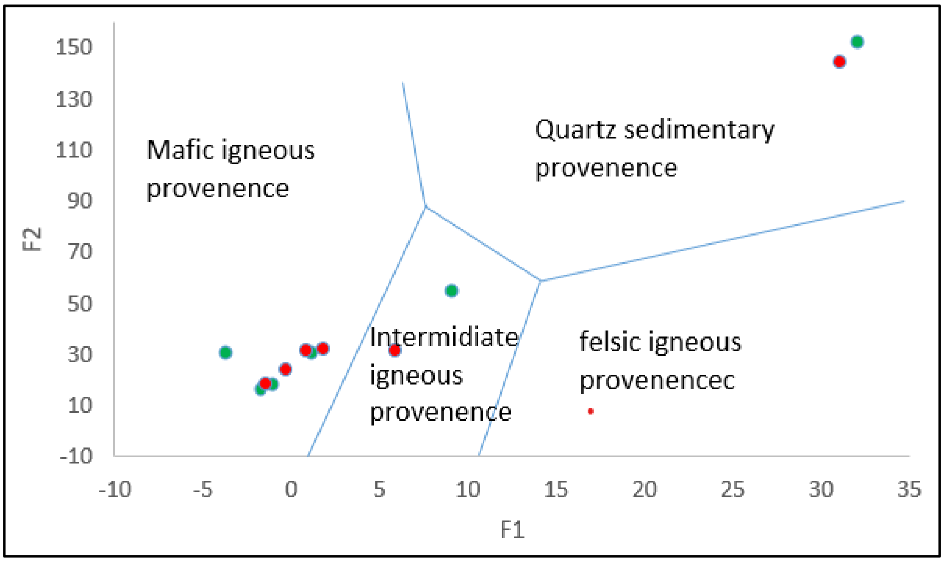

Figure 5. Plot illustrating discriminant scores used to differentiate source signatures; Section A is shown in red, and Section B is shown in green.

The Al2O3/TiO2 ratio commonly points to a sedimentary source, with values between 3 and 8 indicating a mafic igneous source, 8 to 21 suggesting an intermediate source, and 21 to 70 representing a felsic igneous source, respectively (Hayashi et al., 1997). The analyzed samples show a ratio of 9.3 – 23.2 in section A and 11.5 – 26.9 in section B, suggesting a mixed source of intermediate and mafic igneous origin.

Plots of Zr against TiO2 for the analyzed samples indicate that the source is primarily intermediate igneous rocks, with a minor presence of mafic rocks (Figure 6).

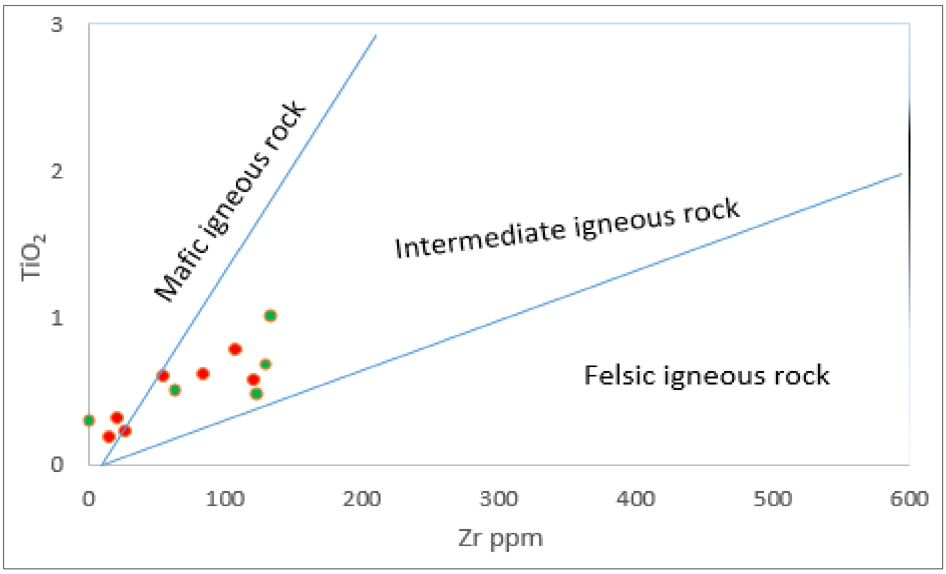

Figure 6. TiO_2-Zr plot for source rock, after (Hayashi et al., 1997). Section A-red color and Section B- green color.

5.4. Paleotectonic Framework

The tectonic setting of clastic rocks within the basins can be determined by using discriminating plots of major and trace elements. Tectonic categorization by Bhatia & Crook (1986) indicates several tectonic settings (island arc, active margin, and passive margin). The SiO_2/Al_2O_3-K_2O/Na_2O diagram by (Roser & Korsch, 1986) displays similar divisions, with passive margin rocks characterized by high values in both ratios, while active margin rocks show a decreasing SiO_2/Al_2O_3 ratio and varying low K_2O/Na_2O ratio (McLennan et al., 1993). As per the (Roser & Korsch, 1986) plot, the clay samples from both sections plot within the fields of passive and active margins (Figure 7).

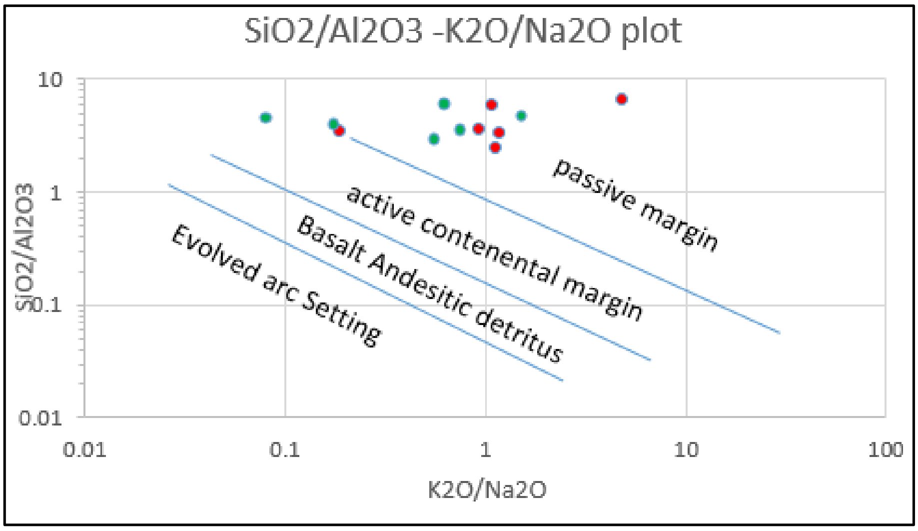

Figure 7. Paleotectonic representative graph, section A in red color and section B in green color.

5.5. Palaeoweathering Environment

The weather conditions, coupled with the movements in the crust of the earth, influence the intensity of rock breakdown and the wearing away of the original rocks. An index to quantify chemical alterations (CIA) = (Al_2O_3/ Al_2O_3+ CaO + Na_2O + K_2O) x100 and an index to quantify chemical wearing (CIW) = molar (Al_2O_3/ [Al_2O_3 + CaO+ Na_2O]) x 100 are useful in the determination of previous weathering activity. CIW and CIA are assumed in the same way, so that a value of approximately 50 is interpreted to mean that there is no weathering, and a value near 100 is interpreted to mean that there is a lot of weathering (Taylor & McLennan, 1985; Nesbitt, 2003). Clay layers of area A (80 – 86.9) and area B (78.7 to 84.6) had a variety of data (CIW) of 80 – 86.9 and 78.7 – 84.6, respectively, which indicated that the original rocks had undergone significant chemical weathering (Table 3).

Table 3. Elemental ratios average of clay samples

Section	*Sr/Cu*	*Rb/Sr*	*Ni/Co*	*V/Ni*	*U/Th*	*V/ (Ni + V)*	*CIA*	*CIW*
A	13.78	0.127	22.7	0.59	0.72	0.36	78.7	84.6
B	15.97	0.12	15.03	1.7	1.1	0.52	80	86.9

5.6. Chemical Maturity and Paleoclimate

The graph of Na vis-a-vis Mg to identify the environment of deposition in ancient times, as proposed by Nicholson (1992), shows that the tested samples are a reflection of a marine environment (Figure 8).

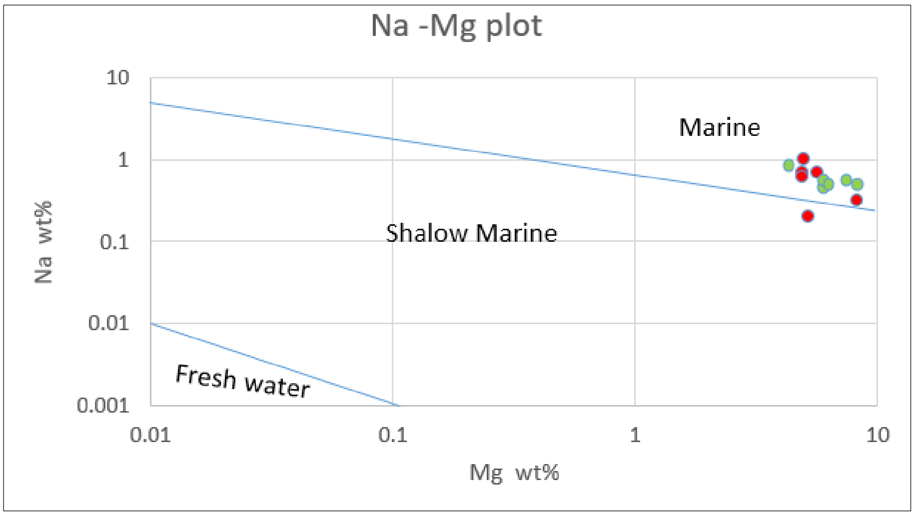

Figure 8. Mg vs Na diagnostic plots show the sedimentary environment for the studied samples after (Nicholson, 1992), section A-red color and section B- green color.

The percentage of SiO_2 /(Al_2O_3 + K_2O +Na_2O) ratio also provides useful information on the ancient weather patterns at the time of sedimentation (Suttner & Dutta, 1986). A two-part diagram of the samples under consideration (Figure 9) indicates primarily wet weather conditions, as well as growing chemical development. This depends on the weather conditions under which settling of sediments takes place, in that warm and wet climates are more favorable to chemical weathering (Rocks, 1968).

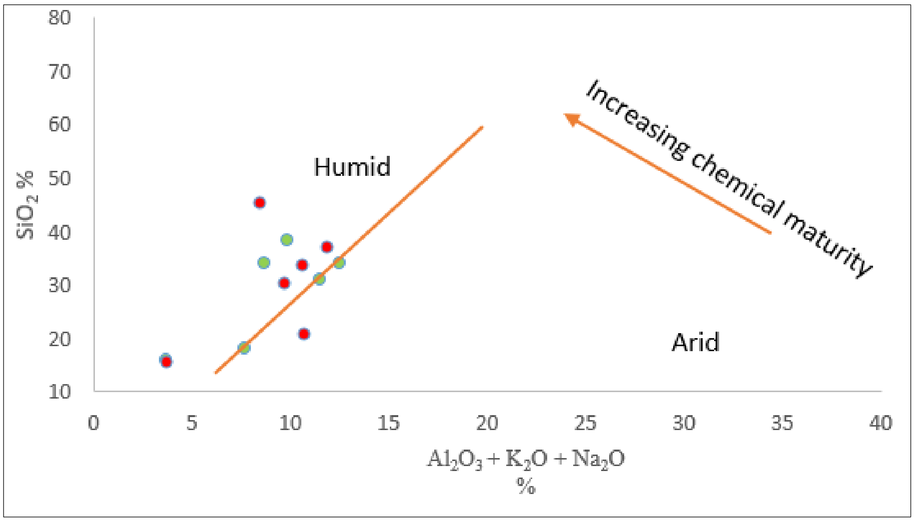

Figure 9. Climate diagram, section A in red color and section B in green color.

Past climate can also be estimated using trace elements. The Sr/Cu ratio of 1.3 – 5 indicates a warm or wet climate, whereas the Sr/Cu ratio above 5.0 is the indication of the hot, dry climate (Tao et al., 2017). On the other hand, a low value of the ratio of Rb/Sr means that there is a dry climate, whereas high values depict a warm climate (Xu et al., 2010). The mean Sr/Cu ratio of the samples analyzed is (13.78 and 15.9) in the samples of area A and B, respectively, indicating a hot dry climate, whereas a low mean value of the Rb/Sr ratio (0.127 to 0.12) in the samples of areas A and B, respectively, indicates a dry climate (Table 3).

5.7. Redox Environments

Various elemental ratios, including U/Th, Th/ U, Ni/Co, V/ Ni, and Cu/Zn, are examined to determine the previous redox conditions during the time that sediments settled. The Ni / Co ratio below 5 indicates that there are oxic conditions, and the ratio above 5 indicates suboxic and anoxic conditions (Bal Akkoca et al., 2019).

The samples that were examined contain Ni/Co values of 22.7 in section A and 15.03 in section B, which indicate a suboxic environment and an anoxic environment (Table 3).

A V/ Ni ratio above 3 is associated with reducing environment, and a V/Ni ratio of 1.9 -3 is associated with suboxic conditions (Galarraga et al., 2008). Sections A and B indicate a suboxic environment with V / Ni levels of 0.59 and 1.7, respectively.

A U/Th ratio of below 1.25 is the indication of an oxic environment, and above 1.25 is the indication of a suboxic and anoxic environment (Nagender Nath et al., 1997). The clay samples in the present study are low in U/Th (0.72 -1.1) in Part A and B, and this indicates an oxic environment (Table 3).

Oxic environments have a V / (N i + V) ratio of lower than 0.46, whereas suboxic and anoxic environments have 0.54 - 0.82 levels and higher (Hatch & Leventhal, 1992). The ratio of clay V / (Ni + V) in sections A and B is 0.36 and 0.52, respectively, indicating the presence of suboxic and anoxic conditions.

6. Discussion of Results

The mineral and chemical composition of sedimentary rocks is largely dependent on some factors, such as the mineral and chemical makeup of the rocks with which they formed, the influence of breaking and erosion, movement, settling, post-depositional changes, and movement of the Earth's crust (McLennan et al., 1993; Dickinson & Suczek, 1979).

Diagrams were utilized based on the likely origin of the rock contents of layered sediments and the ancient structural framework based on the methods suggested by Hayashi et al. (1997) and Roser & Korsch (1986). The sampled ones belonged to the basic and intermediate igneous rock origins, and this condition signifies that there was a diverse source. The samples are in passive and active margin setups. Active-margin sediments typically contain a very low SiO_2/Al_2O_3

ratio and a slightly varying K_2O/Na_2O ratio, whereas passive-margin deposits have higher percentages of the ratios. AP10 is the Middle Palaeocene-Eocene Megasequence, when a new phase of sinking and volcanic activity took place, as the NeoTethys finally closed in. This caused elevation along the NE side of the Arabian Plate, forming ridges and basins which generally extended along the NW – SE directions in the north and center of Iraq, so the E-W direction in western Iraq. Through these structural characteristics, there were major variations in the kinds of rocks (Jassim & Goff, 2006).

Chemical Index Alteration (CIA) and Chemical Index Weathering (CIW) indicate that the original sediments experienced a large level of disintegration. An increase in high CIA values depicts the volume of clay minerals relative to feldspar, which has the capacity to augment the quantity of Al_2O_3 (Oghenekome et al., 2018). The boundary between Paleocene and Eocene is characterized by the diversity of biological, mineralogical, and even chemical factors describing the global transformations of the ancient environment, including the essential alterations of climate (Kender et al., 2012).

The graph presented by (Suttner & Dutta, 1986), SiO_2 wt. per cent vs (Al_2O_3 + K_2O + Na_2O) wt. Per cent shows the historical climatic situation that influenced the deposition of the sediments. The samples of the clay are primarily those of the humid climate, with the elemental ratios of Sr/Cu and Rb/Sr indicating a hot, dry climate. Such changes in ancient climate will have some effects on the chemical component of the source rocks, which will be able to show alteration in the ancient climate at the time of deposition (Gu et al., 2022). The elemental ratios employed to determine the conditions of the primitive environment show that suboxic, anoxic, and oxic conditions might have prevailed in the deposition of sediments. This environment of deposition of the detritus sediments of reducing nature can indicate that an increase in the level of the sea was succeeded by a gradual decrease in the levels during the deposition of the layers analyzed.

Anoxic conditions can take place in basin sediments in two different ways. The former is when the waters of the sedimentary basin are anoxic themselves. The second one is when the speed at which the sediments are covered is greater than the speed at which the dissolved oxygen is restored. Trace and minor elements under oxic, as well as anoxic conditions in the marine environment, are likely to act differently (Calvert & Pedersen, 1993). The ice/oxygen variations between suboxic/anoxic and complete oxic conditions may be associated with the presence of continental input, which may be attributed to non-oxidized rock formation or oxidized rock formations.

The relative deepening of the environment in comparison with the earlier state, as well as the variety of the geological conditions that affect the processes of bed formation, cause the change in the redox conditions, which transforms the oxic to the non-oxic state (Liu et al., 1988).

7. Conclusions

A study on the geochemical composition of the clay layers within the Eocene strata indicates that the major oxides in their average concentration are: SiO_2, CaO, MgO, Al_2O_3, and Fe_2O_3, which are the major building blocks of the clay. In comparison with PAAS and NASC, the concentrations of MgO and CaO increase, but the concentrations of other oxides decrease. The elements in section A are presented in the following order, namely: Mn > Cr > Sr > Ni > V > Zn >Zr >Rb > Co > Th > U, whereas the elements in section B are slightly different in that they are listed as follows: Sr > Mn > Cr > Ni >V > Zn > Zr > Rb > Co > Th > U. As a result, it is possible to use geochemical discrimination diagrams to identify the source rocks and provenance of the mafic igneous, intermediate, and felsic igneous rocks, indicating a heterogeneous source.

As far as multi-elemental diagrams are concerned, it is important to note that passive and active margins are the main cause behind the paleotectonic formation of clay layers and that the application of paleo-weathering conditions implies that clay samples experienced extensive chemical weathering and increased chemical maturity of the source area. The Na vs. Mg plot reveals that it has a marine depositional basin. In regards to the climate, the analysis revealed that with the bivariate plots of the $Al_2O_3 + K_2O + Na_2O$ against the SiO_2 binary diagrams, it would suggest that the climate would likely be humid but the elemental ratios, Sr/Cu and Rb/Sr, suggests a hot, dry climate and in that order, the elemental ratios suggest that the elements could have been under suboxic, anoxic, and oxic conditions when depositing the sediments.

References

Abubakar, U., Usman, M. B., Bello, A. M., Garba, T. A., & Hassan, S. (2019). Geochemical and palaeocurrent analysis of the Tertiary Kerri–Kerri Formation in the Gongola Sub-Basin of the Northern Benue Trough, North-eastern Nigeria: implications for provenance, tectonic setting and palaeoweathering. *SN Applied Sciences*, *1*(10). https://doi.org/10.1007/s42452-019-1196-7

Armstrong-Altrin, J. S., Lee, Y. Il, Kasper-Zubillaga, J. J., & Trejo-Ramírez, E. (2017). Mineralogy and geochemistry of sands along the Manzanillo and El Carrizal beach areas, southern Mexico: implications for palaeoweathering, provenance and tectonic setting. *Geological Journal*, *52*(4). https://doi.org/10.1002/gj.2792

Bal Akkoca, D., Erış, K. K., Çağatay, M. N., & Bıltekın, D. (2019). The mineralogical and geochemical composition of Holocene sediments from Lake Hazar, elazığ, Eastern Turkey: Implications for weathering, paleoclimate, redox conditions, provenance, and tectonic setting. *Turkish Journal of Earth Sciences*, *28*(5). https://doi.org/10.3906/yer-1812-8

Bhatia, M. R., & Crook, K. A. W. (1986). Trace element characteristics of graywackes and tectonic setting discrimination of sedimentary basins. *Contributions to Mineralogy and Petrology*, *92*(2), 181–193. https://doi.org/10.1007/BF00375292

Calvert, S. E., & Pedersen, T. F. (1993). Geochemistry of Recent oxic and anoxic marine sediments: Implications for the geological record. *Marine Geology*, *113*(1–2). https://doi.org/10.1016/0025-3227(93)90150-T

Dickinson, W. R., & Suczek, C. (1979). Plate tectonics and sandstone composition. *American Association of Petroleum Geologists Bulletin*, *63*(12). https://doi.org/10.1306/2f9188fb-16ce-11d7-8645000102c1865d

Fendakly, S. M. (2011). *Facies analysis and sedimentological model of Pila Spi Formation in selected areas from North Iraq.* [Thesis]. University of Mosul-College of Science.

Galarraga, F., Reategui, K., Martïnez, A., Martínez, M., Llamas, J. F., & Márquez, G. (2008). V/Ni ratio as a parameter in palaeoenvironmental characterisation of nonmature medium-crude oils from several Latin American basins. *Journal of Petroleum Science and Engineering*, *61*(1), 9–14.

Gromet, L. P., Haskin, L. A., Korotev, R. L., & Dymek, R. F. (1984). The "North American shale composite": Its compilation, major and trace element characteristics. *Geochimica et Cosmochimica Acta*, *48*(12). https://doi.org/10.1016/0016-7037(84)90298-9

Gu, Y., Hu, D., Wei, Z., Liu, R., Hao, J., Han, J., Fan, Z., Jiang, Y., Wang, Y., & Xu, Q. (2022). Sedimentology and geochemistry of the Upper Permian Linghao Formation marine shale, central Nanpanjiang Basin, SW China. *Frontiers in Earth Science*, *10*, 914426.

Hatch, J. R., & Leventhal, J. S. (1992). Relationship between inferred redox potential of the depositional environment and geochemistry of the Upper Pennsylvanian (Missourian) Stark Shale Member of the Dennis Limestone, Wabaunsee County, Kansas, U.S.A. *Chemical Geology*, *99*(1–3). https://doi.org/10.1016/0009-2541(92)90031-Y

Hayashi, K. I., Fujisawa, H., Holland, H. D., & Ohmoto, H. (1997). Geochemistry of ∼1.9 Ga sedimentary rocks from northeastern Labrador, Canada. *Geochimica et Cosmochimica Acta*, *61*(19). https://doi.org/10.1016/S0016-7037(97)00214-7

Jassim, S. Z., & Goff, J. C. (2006). Geology of Iraq. In *... Printing, Mosul, Iraq*.

Kender, S., Stephenson, M. H., Riding, J. B., Leng, M. J., Knox, R. W. O. B., Peck, V. L., Kendrick, C. P., Ellis, M. A., Vane, C. H., & Jamieson, R. (2012). Marine and terrestrial environmental changes in NW Europe preceding carbon release at the Paleocene-Eocene transition. *Earth and Planetary Science Letters*, *353–354*. https://doi.org/10.1016/j.epsl.2012.08.011

Liu, Y.-G., Miah, M. R. U., & Schmitt, R. A. (1988). Cerium: a chemical tracer for paleo-oceanic redox conditions. *Geochimica et Cosmochimica Acta*, *52*(6), 1361–1371.

McLennan, S. M., Hemming, S., McDaniel, D. K., & Hanson, G. N. (1993). Geochemical approaches to sedimentation, provenance, and tectonics. *Special Paper of the Geological Society of America*, *284*. https://doi.org/10.1130/SPE284-p21

Nagender Nath, B., Bau, M., Ramalingeswara Rao, B., & Rao, C. M. (1997). Trace and rare earth elemental variation in Arabian Sea sediments through a transect across the oxygen minimum zone. *Geochimica et Cosmochimica Acta*, *61*(12). https://doi.org/10.1016/S0016-7037(97)00094-X

Neikov, O. D., Naboychenko, S. S., & Yefimov, N. A. (2018). Handbook of Non-Ferrous Metal Powders: Technologies and Applications, Second Edition. In *Handbook of Non-Ferrous Metal Powders: Technologies and Applications, Second Edition*. https://doi.org/10.1016/C2014-0-03938-X

Nesbitt, H. W. (2003). Petrogenesis of siliciclastic sediments and sedimentary rocks. *Geochemistry of Sediments and Sedimentary Rocks*, *4*, 39–51.

Nicholson, K. (1992). Contrasting mineralogical-geochemical signatures of manganese oxides: guides to metallogenesis. *Economic Geology*, *87*(5), 1253–1264.

Oghenekome, M. E., Chatterjee, T. K., van Bever Donker, J. M., & Hammond, N. Q. (2018). Geochemistry and weathering history of the Balfour sandstone formation, Karoo basin, South Africa: Insight into provenance and tectonic setting. *Journal of African Earth Sciences*, *147*. https://doi.org/10.1016/j.jafrearsci.2018.07.014

Rocks, S. (1968). *Petrology of sedimentary rocks*. Springer.

Roser, B. P., & Korsch, R. J. (1986). Determination of tectonic setting of sandstone- mudstone suites using SiO2 content and K2O/Na2O ratio. *Journal of Geology*, *94*(5). https://doi.org/10.1086/629071

Sissakian, V. K., & Fouad, S. F. (2016). Geological map of Sulaimaniyah quadrangle, at scale of 1: 250 000. *Journal of Zankoy Sulaimani - Part A*, *GeoKurdistan II*(Special issue). https://doi.org/10.17656/jzs.10477

Suttner, L. J., & Dutta, P. K. (1986). Alluvial sandstone composition and paleoclimate; I, Framework mineralogy. *Journal of Sedimentary Research*, *56*(3), 329–345.

Tao, S., Xu, Y., Tang, D., Xu, H., Li, S., Chen, S., Liu, W., Cui, Y., & Gou, M. (2017). Geochemistry of the Shitoumei oil shale in the Santanghu Basin, Northwest China: Implications for paleoclimate conditions, weathering, provenance, and tectonic setting. *International Journal of Coal Geology*, *184*. https://doi.org/10.1016/j.coal.2017.11.007

Taylor, S. R., & McLennan, S. M. (1985). The Continental Crust: Its Composition and Evolution. An Examination of the Geochemical Record Preserved in Sedimentary Rocks. In *The Continental Crust: Its Composition and Evolution. An Examination of the Geochemical Record Preserved in Sedimentary Rocks.*

Wronkiewicz, D. J., & Kent C, C. (1989). Geochemistry and provenance of sediments from the Pongola Supergroup, South Africa: Evidence for a 3.0-Ga-old continental craton. *Geochimica et Cosmochimica Acta*, *53*(7). https://doi.org/10.1016/0016-7037(89)90236-6

Xu, H., Liu, B., & Wu, F. (2010). Spatial and temporal variations of Rb/Sr ratios of the bulk surface sediments in Lake Qinghai. *Geochemical Transactions*, *11*(1), 3.